Grafting of Poly(alkyl (meth)acrylates) from Swellable Poly(DVB80-*co*-HEMA) Microspheres by Atom Transfer Radical Polymerization

Guodong Zheng and Harald D. H. Stöver*

Department of Chemistry and Brockhouse Institute for Materials Research, McMaster University, Hamilton, Ontario, Canada L8S 4M1

Received March 18, 2002

ABSTRACT: We report the graft polymerization of methyl acrylate (MA), methyl methacrylate (MMA), hydroxyethyl methacrylate (HEMA), and 2-(dimethylamino)ethyl methacrylate (DMAEMA) by atom transfer radical polymerization (ATRP) from lightly cross-linked poly(DVB80-*co*-HEMA) microspheres. These poly(DVB80-*co*-HEMA) microspheres were prepared by precipitation copolymerization and subsequently modified by reaction with 2-bromopropionyl bromide to serve as ATRP macroinitiators. MMA, MA, and HEMA were then grafted from these initiator microspheres at room temperature using CuBr/Me_4cyclam as catalyst. The graft sites, and hence the grafted polymers, are distributed throughout the initiator microspheres. Addition of a second monomer formed grafted block copolymers, indicating that a significant portion of the first grafts could be reactivated. The final particles represent novel, high-capacity polymer supports comprised of swellable core particles carrying 5.09 and 5.18 mmol/g of grafted poly(DMAEMA) and poly(MMA-*b*-DMAEMA), respectively. The grafted particles were characterized using ESEM, FTIR, Coulter particle sizing, and potentiometric titration.

Introduction

Polymer-supported reagents, scavengers, and catalysts have been successfully used in organic synthesis.[1] Advantages such as high product purity, and simplification of workup in high-throughput parallel synthesis, continue to drive the development of new polymer-supported reagents.[2] The majority of supported reagents are based on divinylbenzene (DVB) cross-linked polystyrene (PS), which is very stable in both basic and acidic media and in all organic solvents.[3] However, lightly cross-linked polystyrene resins must be swollen in good solvents before use to allow penetration by the reactant. They perform badly in poor solvents for PS, which are required in some syntheses. Bayer[4] grafted poly(ethylene glycol) (PEG) onto lightly cross-linked polystyrene beads by anionic polymerization, forming the so-called TentaGels. At high PEG loadings, these TentaGel beads swell in all solvents dissolving PEG. The resulting PEG-grafted polymer-supported reagents are suitable for reactions in a wide range of solvents, including the solid-phase supported synthesis of peptides and nucleotides. Because of the use of anionic polymerization in the graft polymerization, the desired functional groups could only be introduced at the termini of the PEG chains, and consequently, the functional capacity of TentaGel resins is fairly low.

If the functional groups were present in every monomer unit of the grafted polymer, the capacity of the resulting polymer-supported reagents would be greatly increased and could lead to polymer-supported reagents combining a high swelling factor and a high functional capacity. So far, polymer-supported reagents with such combined properties are unavailable. Bradley et al.[5] tried to enhance the functional capacity of solid supports using a dendrimerization process. Three generations of amidoamino dendrimers were built on a TentaGel base with a modest increase in amine loading from 0.85 to 4.0 nmol/bead.

Recently, atom transfer radical polymerization (ATRP), a controlled/living polymerization, has been developed.[6] The livingness of ATRP allows sequential polymerization of monomers to produce block copolymers. Matyjaszewski et al.[7] have demonstrated the controlled ATRP of (meth)acrylates from monofunctional narrow-disperse poly(dimethylsiloxane) (PDMS) macroinitiators. The resulting polymers showed linear increases in number-average molecular weight (M_n) with conversion, demonstrating the effectiveness of ATRP in synthesizing a variety of inorganic/organic polymer hybrids. Jérôme et al.[8] used difunctional poly(*n*-butyl acrylate) as a macroinitiator for the polymerization of methyl methacrylate (MMA) to produce poly(MMA-*b*-BA-*b*-MMA) triblock copolymers with a polydispersity index of 1.15.

Typically, ATRP initiators are halide compounds, such as benzyl halides and α-halo carboxylates, which convert into stabilized radicals upon halide transfer. The growth of polymer chains from the initiator is activated by metal complexes. The ability to grow polymer chains from halide initiators has been used for grafting polymer off solid surfaces. Porous silica gel coated with a self-assembled monolayer from 1-trichlorosilyl-2-(*m*/*p*-chloromethylphenyl)ethane successfully initiated polymerization of acrylamide. The number-average molecular weights of the grafted polymers were up to 13−15 kDa, with PDI's below 1.3.[9] Polystyrene with M_n = 26 500 and PDI = 1.33 was also grafted from silica nanoparticles via ATRP, leading to an increase in the diameter of the nanoparticles by about 20 nm.[10] We recently introduced 1-chloroethylbenzene initiators onto poly-DVB particles by hydrochlorination of residual vinyl groups, and conducted ARTP of styrene from the initiator sites located on and below the particle surface, to produce polystyrene grafted particles with a greater than 100 nm increase in diameter.[11]

Another advantage of ATRP is its tolerance to water and many functional groups,[12] which makes it ideal for use with functional monomers. We hence planned to

10.1021/ma020421w CCC: $22.00
Published on Web 08/24/2002

Scheme 1. Reaction of Bromopropionyl Bromide with Precursor Particles H_i To Produce Initiator Particles H_iBr and the Subsequent Graft-Polymerization and Graft-Block Copolymerization of Alky (Meth)acrylates from H_iBr

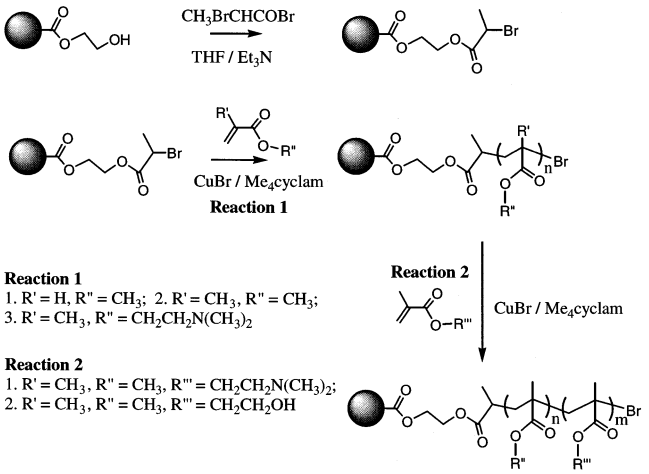

introduce functional groups in every monomer unit in a grafted polymer to prepare high-capacity polymer-supported reagents.

A key aspect of this plan was to graft polymer from lightly cross-linked particles. These precursor particles could be prepared by a precipitation copolymerization of divinylbenzene (DVB) and hydroxyethyl methacrylate (HEMA). These particles can be designed to have a relatively highly cross-linked core and a lightly cross-linked outer layer due to the difference in reactivity between DVB and HEMA. The hydroxyl group in HEMA would be reacted with α-bromopropionyl bromide to generate an ATRP initiator. Polymer chains could then be grown from the initiator sites located in the outer layers and at the surface of the particles (Scheme 1).

Experimental Section

Chemicals. DVB80 (70−85% DVB isomers, Fluka, Oakville, Canada), 1,4,8,11-tetramethyl-1,4,8,11-tetraazcyclotetradecane (Me_4cyclam) (98%, Aldrich), acetonitrile (HPLC grade, Aldrich), 2-bromopropionyl bromide (97%, Aldrich) and triethylamine (99%, Aldrich) were used as received. 2,2′-Azobis(2-methylpropionitrile), AIBN (Eastman Kodak Co.), was recrystallized from methanol. Hydroxyethyl methacrylate (HEMA) (97%), methyl methacrylate (MMA) (99%), and 2-(dimethylamino)-ethyl methacrylate (DMAEMA) (98%) were purchased from Aldrich Chemical Co. and purified by distillation under vacuum prior to polymerization. THF (99+%, Aldrich) was refluxed over K−Na alloy and distilled under nitrogen. CuBr was prepared by the reaction of $CuBr_2$ with dimethyl malonate.[11]

Methods. *Preparation of Precursor Particles.* Precursor particles, poly(DVB80-*co*-HEMA), were prepared by precipitation polymerization in neat acetonitrile. DVB80 (1.05 g, 8 mmol), HEMA (4.95 g, 38 mmol), acetonitrile (200 mL), and AIBN (0.12 g) were placed in a 250 mL polyethylene bottle and shaken vigorously to ensure complete dissolution of the initiator. The bottle was placed in a reactor equipped with horizontal rollers and a programmable temperature controller. The reactor gently agitates the sample by rolling the bottles at approximately 4 rpm. The temperature profile used for polymerization started with a 1 h ramp from room temperature to 60 °C followed by a 100 min ramp to 70 °C and then a further 24 h at 70 °C. The resulting particles were isolated by vacuum filtration over a 0.5 μm membrane filter with three subsequent washings with THF. The yield of clean particles was 3.04 g (50.7%) after drying at room temperature under vacuum for 24 h.

Preparation of Initiator Particles. Precursor particles (2.00 g) were suspended for 2 h in 20 mL of THF containing 0.95 g (9.39 mmol) of triethylamine in a 50 mL two-necked round-bottomed flask, followed by dropwise addition of 2.0 g (9.26 mmol) of 2-bromopropionyl bromide to the suspension, which was cooled with an ice−water bath. The mixture was stirred at room temperature overnight. The initiator particles were filtered and washed with THF and methanol thoroughly. The yield of the resultant particles was 3.08 g after drying at room temperature under vacuum for 24 h.

Grafting Polymers from Particles. The ATRP was carried out in THF solution. Initiator particles (H_1Br, 0.3 g) and methyl methacrylate (2.0 g, 20 mmol) were dissolved in 8 mL of THF in a 25 mL flask purged with THF saturated nitrogen for 1 h, and then a degassed 2 mL THF solution of CuBr (26 mg, 0.18 mmol)/Me_4cyclam (46 mg, 0.18 mmol) was added via a cannula. The mixture was stirred with a magnetic bar at room temperature under nitrogen for 15 h. The resulting blue particles were centrifuged and redispersed at least three times in THF and then repeatedly in methanol until the particles became almost white. The yield of poly(MMA) grafted particles was 1.24 g.

The progress of the polymerization was tracked by removing aliquot samples with a syringe at various time intervals. The samples were centrifuged and purified as described above.

Grafting Block Copolymers from Particles. A similar procedure was used to graft the second generation poly(DMEAMA) or poly(HEMA) from particles already grafted with the first generation poly(MMA). The poly(MMA) grafted particles (H_1-Br-*g*-poly(MMA), 0.3 g) and HEMA (1.5 g, 11.5 mmol) were dissolved in 8 mL of THF in a 25 mL flask purged with THF saturated nitrogen for 1 h, and then a degassed 2 mL THF solution of CuBr (5.8 mg, 0.04 mmol)/Me_4cyclam (10.2 mg, 0.04 mmol) was added via a cannula. The polymerization was conducted at room temperature for 23 h. The yield of block copolymer grafted particles was 1.03 g.

Particle Size Analysis. The particle sizes and size distributions were measured using a 256-channel Coulter Multi-Sizer II interfaced with a computer. A 50 μm aperture tube was chosen to accommodate the particles size range of 1−7 μm. A small amount of particles dispersed in acetone was added to 25 mL of Coulter Isoton II electrolyte solution and stirred for 1 min. The Coulter Multi-Sizer II measurements were confirmed using a Philips ElectroScan 2020 environmental scanning electron microscope (ESEM). The samples for ESEM were prepared by dispersing particles in THF and casting a drop of particle suspension onto pieces of glass. The samples were dried under vacuum for 2 h and sputter-coated with 5 nm of gold.

TEM Analysis. The internal structure of the grafted particles was studied using a JEOL 1200EX transmission electron microscope. Here, the samples were embedded in Spurr epoxy resin and microtomed to generate 40−60 nm thick slices.

FT-IR Analysis. Fourier transform infrared analysis was performed on a Bio-Rad FTS-40 FT-IR spectrometer. All samples were prepared as pellets using spectroscopic grade KBr in a Carver press at 15 000 psi. The spectra were scanned over the range 4000−400 cm^{-1}, in the transmission mode, at a resolution of 2 cm^{-1}.

Results and Discussion

Preparing Precursor Particles with Hydroxyl Groups and Initiator Particles. Particles with hydroxyl groups were prepared by a precipitation copolymerization of DVB80 and HEMA in acetonitrile. The formation of particles and their size and size distribution are strongly dependent on the monomer loading and cross-linker ratio. As we wish to prepare lightly cross-linked particles, different ratios of cross-linker (DVB80) to HEMA were selected to optimize the polymerization conditions to reach monodispersed particles with low

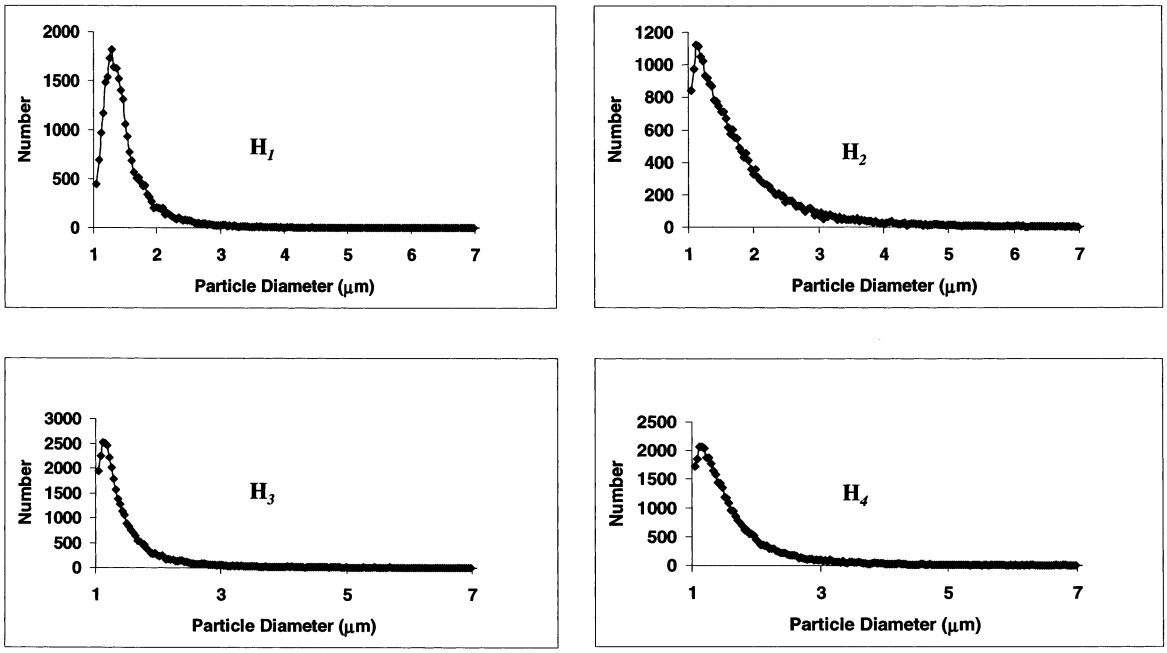

Figure 1. Size and size distribution of precursor particles having different ratios of HEMA to DVB80: H_1 (82.5 mol % HEMA); H_2 (73.2 mol % HEMA); H_3 (63.8 mol % HEMA); H_4 (54.0 mol % HEMA).

cross-link degrees. The different cross-linker ratios led to differences in the size and size distribution of the particles. Figure 1 shows the size distributions for four different samples as measured by a Coulter Multi-Sizer II. The lowest cross-linker ratio (sample H_1, 82.5 mol % HEMA) gave large particles with narrow size distribution. Further decreasing the cross-linker content resulted in the formation of coagulum instead of particles.

The particles H_1 with 82.5 mol % fraction of HEMA should have the highest swelling ratio and the highest hydroxyl groups content, which should allow the introduction of more initiators per particle. The efficiency of cross-linking in precipitation polymerization usually is much lower than in emulsion or suspension polymerization, due to the low total monomer loadings used here. This results in an actual cross-linking degree up to an order of magnitude lower than the cross-linker fraction in the monomer. In the present case, the residual pendant vinyl groups may lead to secondary cross-linking during the subsequent graft polymerization. The overall cross-linking degree should decrease from the particle center to the shell, due to the tendency of styrenic and methacrylic monomers to form alternating copolymers. Although the monomer reactivity ratios for copolymerization of DVB and HEMA are not available, comparison with the parent comonomer pair of styrene and methyl methacrylate, which have monomer reactivity ratios of $r_1 = 0.52$ and $r_2 = 0.46$,[13] is instructive. It implies that the particles H_1 have a higher DVB content in the center and a lower DVB content in the outer layer of the particles. Such particles with lower cross-linker density in the outer layer might be expected to swell more in good solvents than particles with uniform structure.

For comparison, 2 g each of two types of particles H_1 (82.5 mol % HEMA) and H_3 (63.8 mol % HEMA) were used to prepare initiators by esterification of the hydroxyl groups with 2-bromopropionyl bromide. The yields of the two initiator particles H1Br and H_3Br were 3.08 and 2.42 g, respectively, which indicated higher initiator concentration in H_1Br than that in H_3Br. The efficiency of these esterifications in precursor particles H_1 and H_3 can be estimated as 81.2% and 65.2%, respectively, assuming that the precursor particles have compositions equal to the comonomer ratio used to prepare the particles, 82.5% and 63.8% HEMA. In fact, because of the moderate conversion to polymer particles of about 50% commonly seen in the precipitation polymerization, and the slight tendency toward alternating copolymerization of the two monomers, the HEMA fraction in the precursor particles might be slightly lower than in the feed. Therefore, the efficiency of the esterification may have been even higher. The higher conversion observed for H_1 is attributed to easier diffusion of bromopropionyl bromide into the more lightly cross-linked particles.

Grafting MMA and MA from the Initiator Particles. The CuBr/Me_4cyclam catalyst system has proven very effective for the ATRP of *N*,*N*-dimethylacrylamide at room temperature.[14] It should hence also act as a catalyst for (meth)acrylate polymerization as the activation in ATRP depends on the redox reaction of the initiator with the Cu(I) complex. Specifically, 2-bromo-2-methylpropionate should be easier to reduce than 2-bromo-2-methylpropionamide since the ester is a stronger electron-withdrawing group than amide. The initiator particles H_1Br and H_3Br were therefore used to initiate polymerization of MMA and MA. The polymerizations took place in THF solution at room temperature, and the results are shown in Table 1.

The ATRP of MMA from 0.3 g each of H_1Br and H_3Br initiator particles caused weight increases to 1.24 and 0.36 g, or by 313% and 20%, respectively. This result is consistent with the higher initiator loading and accessibility of H_1Br compared with H_3Br. The ATRP of MA from H_1Br and H_3Br gave weight increases of only 157% and 10%, respectively, indicating that the ATRP of MMA is more efficient than that of MA. The dormant 2-bromo-2-methylpropionate end group formed in the polymerization of MMA is easier to activate than the 2-bromopropionate formed in the polymerization of

Table 1. ATRP Polymerization of MMA or MA on Initiator Particles

	inititor particles [0.3 g]	CuBr (mg)/ Me_4cyclam (mg)	monomer[a]	yield (g)[b]
H_1Br-*g*-poly(MMA)	H_1Br	26/46	MMA	1.24
H_1Br-*g*-poly(MA)	H_1Br	26/46	MA	0.77
H_2Br-*g*-poly(MMA)	H_3Br	26/46	MMA	0.36
H_2Br-*g*-poly(MA)	H_3Br	26/46	MA	0.33

[a] 2 g of monomer in 10 mL of tetrahydrofuran. [b] Reaction time, 15 h; temperature, rt.

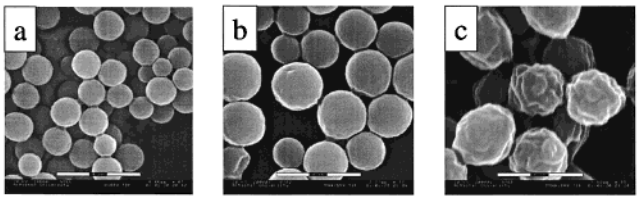

Figure 2. ESEM images of ATRP particles made from initiator particles H_1Br: (a) particles H_1Br; (b) poly(MA) grafted particles H_1Br-*g*-poly(MA); (c) poly(MMA) grafted particles H_1Br-*g*-poly(MMA). The scale bar is 4 μm.

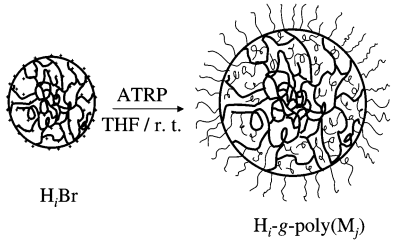

Figure 3. Illustration of internal structure of initiator particles H_iBr and polymer grafted particles.

MA because a more stable tertiary radical is formed. Faster polymerization of MMA was also indicated by a faster change in solution color from gray [Cu(I)] to faint blue [Cu(II)], since the concentration of [Cu(II)] is directly proportional to the concentration of radicals and builds up during the reaction through radical coupling or disproportionation.The size and morphology of the particles were studied by ESEM. Three typical images of grafted particles H_1Br-*g*-poly(MMA), H_1Br-*g*-poly(MA), and H_1Br are shown in Figure 2. After grafting with MMA and MA, the sizes of the particles increased from 1.4 μm to 2.7 and 2.2 μm, respectively. These large size increases confirm that polymer chains not only grow from the surface but also predominantly grow from initiator sites within the particles, as expected from the swellable nature of the initiator particles. Polymerization just of the surface initiator sites would lead to much smaller size increases, on the order of 50−100 nm.

As discussed above, the initiator particles should have a gradient of initiator concentration, increasing from the inside to the surface. As a result, the grafted polymer grown from initiator sites distributed within the initiator particles would form an interpenetrating network with the DVB/HEMA of the original initiator particle and lead to a substantial overall size increase. This interpenetrating network would also show a compositional gradient, based on higher initiator concentration and accessibility near the particle surface. These features are illustrated in Figure 3 for an initiator particle grafted with PMMA. We are currently studying these compositional gradients using scanning transmission X-ray microscopy (STXM).

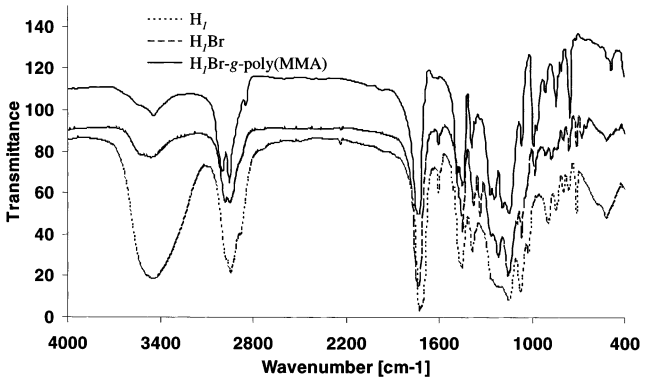

Figure 4. FT-IR spectra of particles. H_1: poly(DVB80-*co*-HEMA) particles made from 82.5 mol % HEMA. H_1Br: initiator particles made from H_1. H_1Br-*g*-poly(MMA): poly(MMA) grafted from particles H_1Br.

The final sizes of the particles H_1Br-*g*-poly(MMA) and H_1Br-*g*-poly(MA) correspond to about 620% and 290% increases in particle volume. However, the weight increases of the particles H_1Br-*g*-poly(MMA) and H_1Br-*g*-poly(MA) were only 313% and 157%. The difference between weight and volume increases suggests that the grafted particles have much lower densities than the initiator particles. Since PMMA and PMA both have inherent densities similar to those of poly(DVB-*co*-HEMA), the difference between weight increase and volume increase must be attributed to an increase in porosity of the resultant particles.

The H_1Br-*g*-poly(MMA) particles have very rough surfaces compared with the H_1Br-*g*-poly(MA) particles. Since PMMA is radiation sensitive,[15] it may depropagate under the electron beam during an ESEM measurement. This would selectively cleave the grafted PMMA from the interpenetrating network and cause the observed rough surfaces. Careful ESEM observation indeed showed that the PMMA-grafted particles do have smooth surfaces when the electron beam is first focused on the particles but that the surface rapidly becomes rough during image acquisition. This depropagation of PMMA in the network also caused a decrease in size and particle volume where the electron beam was focused on the particles, especially at high magnification, suggesting a collapse of the internal pore structure as well. In contrast to PMMA, the PMA-grafted particles were relatively resistant to e-beam damage and showed smooth particle surfaces. This agrees with the results of Cook et al.,[16] who found the monomer concentration of MMA to be 10^6 times higher than that of MA in polymerization−depolymerization equilibria at 25 °C.

Study of Grafted Particles by FT-IR. FT-IR was used to follow the chemical changes occurring during introduction of initiators and the grafting polymerization. Figure 4 shows the FT-IR spectra of precursor particles H_1, initiator particles H_1Br, and the PMMA-grafted particles H_1Br-*g*-poly(MMA). The hydroxyl groups in H_1 give a broad stretching band at 3445 cm^{-1}, and the ester groups give rise to a strong stretching band at 1725 cm^{-1}. In addition, absorptions at 1605 and 1511 cm^{-1} are due to aromatic carbon−carbon double-bond stretching.

In the spectrum of H_1Br, the band at 3445 cm^{-1} due to hydroxyl is dramatically decreased as a result of esterification. The residual hydroxyl absorption, still visible after vacuum-drying the particles for 24 h, indicates that some hydroxyl groups inside particles

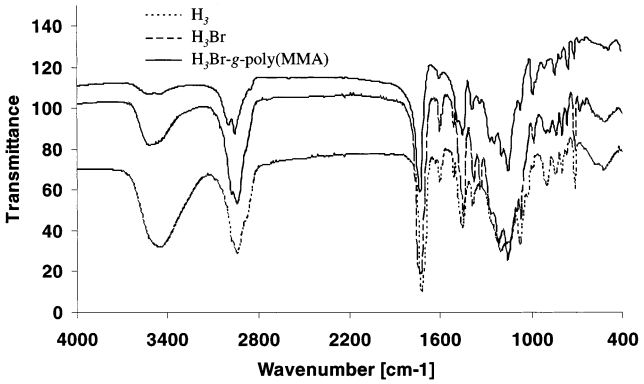

Figure 5. FT-IR spectra of particles. H_3: poly(DVB80-*co*-HEMA) particles made from 63.8 mol % HEMA. H_3Br: initiator particles made from H_3. H_3Br-*g*-poly(MMA): poly(MMA) grafted from particles H_3Br.

were not available for reaction with 2-bromopropionyl bromide. Meanwhile, the characteristic ester carbonyl peak shifted from 1725 cm^{-1} (HEMA) to 1736 cm^{-1} as expected for an α-bromo-substituted ester. The electron-withdrawing bromine at the α-position of the ester in the initiator shifts the carbonyl band to higher wavenumbers compared with the carbonyl band in HEMA. The new absorption at 1339 cm^{-1} was attributed to the methyl group in the initiator,[17] which could be an indicator for ATRP since it should decrease or disappear after polymerization.

After grafting, the carbonyl stretching band in the spectrum of H_1Br-*g*-poly(MMA) is dominated by PMMA, and the peak shifts back to 1727 cm^{-1}. Although grafted PMMA has similar spectral characteristics to the core PHEMA in H_1Br, the changes in relative intensities demonstrate that grafting was successful: (1) the hydroxyl stretching band becomes even smaller as the relative concentration of residual OH groups decreases upon grafting of PMMA, and (2) the aromatic carbon−carbon double-bond stretch at 1605 and 1511 cm^{-1} disappeared in the noise after grafting.The FT-IR spectra of H_3, H_3Br, and H_3Br-*g*-poly(MMA) shown in Figure 5 show similar trends. However, the intensity of the hydroxyl group absorption in H_3Br was larger compared with that of H_1Br, indicating a higher concentration of residual hydroxyl groups in H_3Br. This is likely a result of reduced swelling in the more highly cross-linked H_3, which directly affects the accessibility of reagents.

Absorption due to the benzene rings in the core of the particle is evident in the H_3Br-*g*-poly(MMA) spectrum and is stronger still in the H_3Br-*g*-poly(MA) spectrum. The intensities of the benzene adsorption bands are related to the shell thickness of the particles, which vary in the order of H_1Br-*g*-poly(MMA) > H_1Br-*g*-poly(MA) > H_3Br-*g*-poly(MMA) > H_3Br-*g*-poly(MA), as determined by both diameter and weight increases.

The Living Nature of Graft-ATRP from Particles. The living nature of ATRP allows controlled polymer growth and the production of block copolymers. The living nature of the ATRP in the present graft system was determined by monitoring particle size changes, both with reaction time and with different monomer loadings at constant reaction time. The preparation of block copolymers on particles grafted with poly(MMA) was also used to show the living nature. The ATRP of MMA from initiator particles H_1Br leads to an increase of particle size with reaction time. Figure 6 shows the size distributions of grafted particles over time. The particle size changed significantly with the reaction time. The small peaks appearing to the right of the main peaks during the reaction are attributed to temporary aggregates of 2, 3, or more particles during passage through the Coulter Multi-Sizer orifice, and hence the size and size distributions were calculated using only the main peak. Similarly, the particle volumes were calculated from the main particle diameter. They are plotted as a function of reaction time in Figure 7a.The average particle volume increased rapidly from 1.35 to 4.06 μm^3 during the early stages of polymerization, followed by a slower, linear increase with reaction time. This demonstrates that the size of particles could be controlled through reaction time, especially after the early stages. As discussed above, polymer chains grow from both the surface and interior of the particles. Most polymer chains should be inside the network. The size jump at early stages might be due to the rapid polymerization of monomer within the network of the swollen particle initiator, followed by rapid swelling by solvent. The CuBr/Me_4cyclam catalyst used in this experiment is very efficient, and some polymerizations are complete within minutes.[18] When monomers within the network were consumed, the polymerization rate might be determined by the diffusion of monomer into the network. In addition, the Cu(II)Br concentration would increase after the early stages and promote the formation of dormant species, which would slow the polymerization.

Similarly, particle size could be controlled through monomer loading. The growth of particles with different monomer loading over 15 h reaction time is plotted in Figure 7b. The sizes of the grafted particles at all monomer loadings are significantly larger than that of the initiator particles. The size increase of grafted particles with monomer loading is linear.

Figure 8 shows ESEM images of grafted particles with increase of monomer loadings. No outsized particles were observed in the images, which confirmed the peaks to the right of the main peak in Figure 6 were due to temporary particle aggregates in aqueous solution during measurement. The observed particle surfaces became rougher with higher monomer loading, and with longer reaction time, either due to loss of MMA under the e-beam or due to an amplification of small inhomogeneities of the initiator particles during grafting.

The internal structure originally proposed for the grafted particles, and illustrated in Figure 3, was confirmed by TEM images of microtomed particles (Figure 9**)**. The surface layer of the particles, which consists of almost pure linear PMMA, decomposed under the electron beam and left a void indicated by a white ring. Decomposition was observed when the electron beam was focused on the particle slices. The white rings were present at the beginning but grew with exposure to the electron beam. Also, the white ring was hard to detect for particles with a low degree of MMA grafting.

Grafting Block Copolymer onto Particles. The poly(MMA)-grafted particles obtained after 4 h of polymerization, isolation, and purification were used as initiator particles for a second ATRP of HEMA and DMAEMA. The particle weights increased by 243% (48% conversion of monomer) and 435% (87% conversion of monomer), respectively, upon this second generation grafting at room temperature for 23 h, while the size of the particles increased from 2.7 μm to ca. 4.1 and 4.7

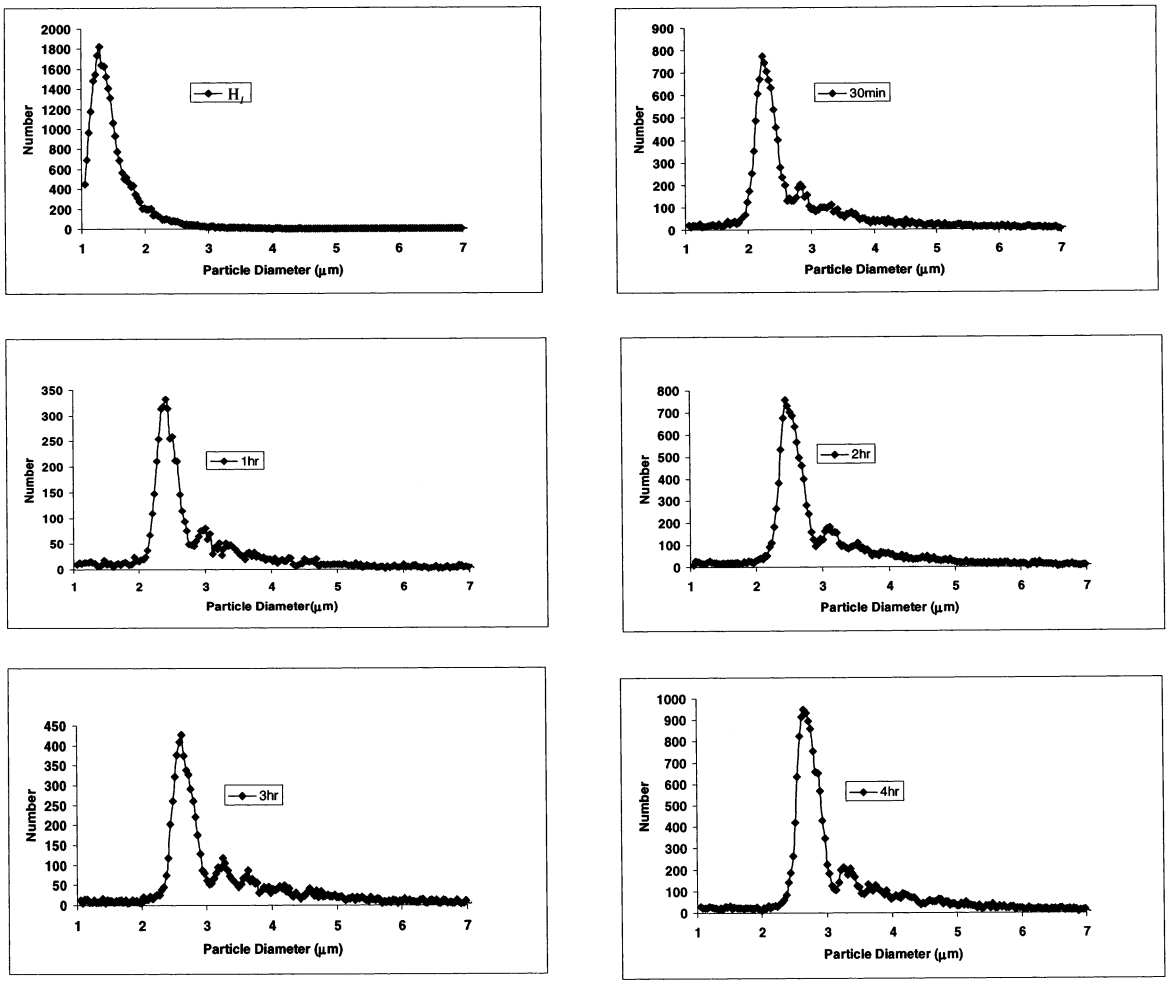

Figure 6. Size and size distribution of H_1Br-*g*-poly(MMA) particles formed by grafting polymerization of MMA for different times.

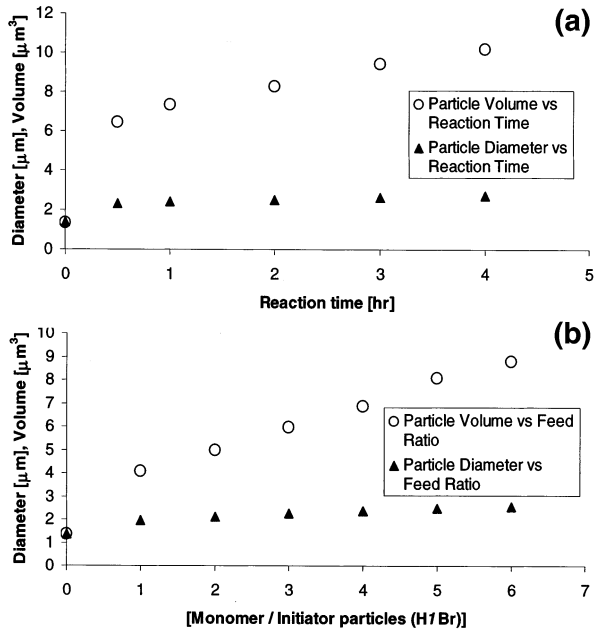

Figure 7. Growth of grafted particles: (a) with different polymerization times at constant monomer feed concentration and (b) with different monomer loading for 15 h. The particle volumes were calculated from the radii using $V = {}^4/_3\pi r^3$.

μm. This result confirmed that a significant portion of the first grafts can be reactivated using ATRP catalysts.

Grafting Functional Polymer onto Particles. Functional polymers containing basic groups were prepared by grafting poly(DMAEMA) onto 0.4 g of H_1-Br particles. A procedure similar to that used to graft MMA and MA onto particles was used. The resulting particles H_1Br-*g*-poly(DMAEMA) showed weight increases of 398% (1.99 g, 80% monomer conversion). The loading of tertiary amine groups on the particles can be calculated from the weight increase after grafting. The functional loading of H_1Br-*g*-poly(DMAEMA) and H_1Br-*g*-poly(MMA)-*b*-poly(DMAEMA) particles was also measured by potentiometric titration with acid. Table 2 compares the functional loadings calculated from the particle weight increase upon grafting with those obtained by potentiometric titrations. The titrations were carried out in aqueous phase and were complete within 10 min. These results confirm the high functional loadings expected from grafting functional monomers off a swellable support resin. In addition, the agreement between weight gain and titration, especially for the graft-block copolymer, indicates that most of the functional groups are highly accessible.

Several factors such as high functional group loading, high polarity, and narrow size distribution should make these particles compatible with proteins and other biomaterials. In the future, we will explore applications in binding and separation of proteins and other biomolecules.

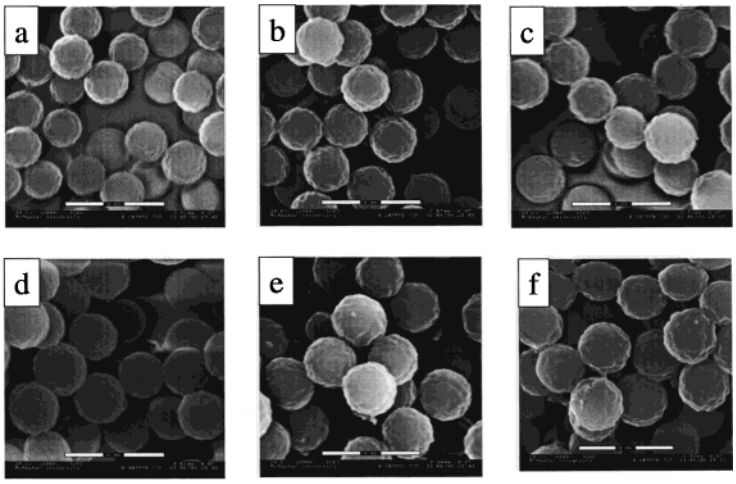

Figure 8. ESEM images of ATRP grafted particles from initiators H_1Br with different monomer loading for 15 h. Grafting polymerization condition: (a) 0.1 g of MMA; (b) 0.2 g of MMA; (c) 0.3 g of MMA; (d) 0.4 g of MMA; (e) 0.5 g of MMA; (f) 0.6 g of MMA. The scale bar is 4 μm.

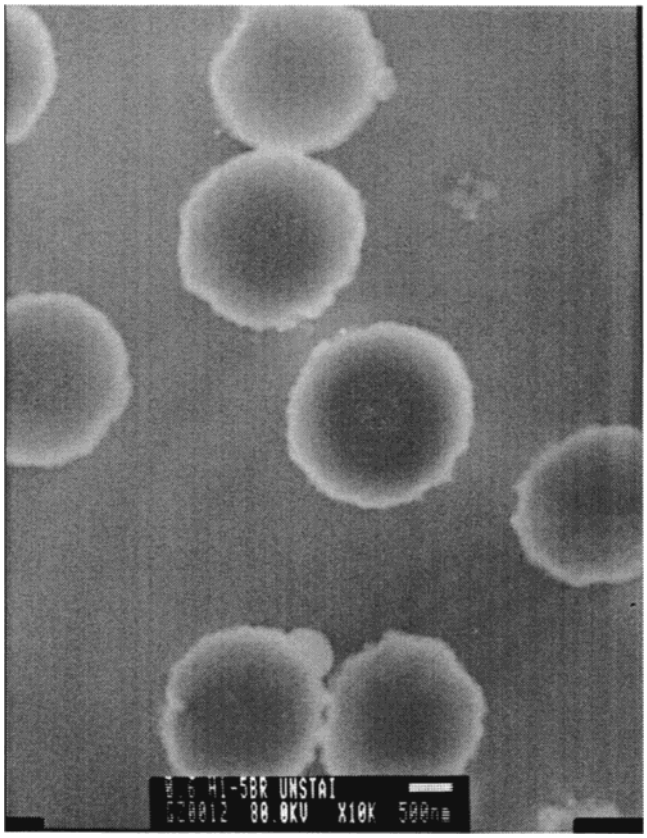

Figure 9. TEM images of poly(MMA) grafted particles from initiators H_1Br. The scale bar is 500 nm.

Table 2. Functional Loading of Grafted Particles

	H_1Br-*g*-poly(DMAEMA)	H_1Br-*g*-[poly(MMA)-*b*-poly(DMAEMA)]
weight increase [g][a]	1.59	0.87
functional loading [mmol/g][b]	5.09	5.18
capacity mmol/g][c]	4.60	5.30

[a] Weight of H_1Br initiator particles: 0.4 g. [b] Based on weight increase. [c] Based on potentiometric titration.

Conclusion

Grafting functional acrylates and methacrylates by controlled/living ATRP from swellable microsphere initiators can lead to novel, highly functional polymer supports. Cu(I)/Me4cyclam serves as an active catalyst of these monomers in THF at room temperature and is suitable for the formation of grafted block copolymer. The original, lightly cross-linked core particles are converted into swellable, interpenetrating network microspheres comprised mainly of the grafted polymer.

Acknowledgment. We thank the National Science and Engineering Research Council of Canada for supporting this research and Dr. Nick Burke for valuable discussions and suggestions. G.Z. thanks the Department of Chemistry at McMaster University for its financial support.

References and Notes

(1) Shuttleworth, S. J.; Allin, S. M.; Sharma, P. K. *Synthesis* **1997**, 1217−1239.

(2) Ley, S. V.; Baxendale, I. R.; Bream, R. N.; Jackson, P. S.; Leach, A. G.; Longbottom, D. A.; Nesi, M.; Scott, J. S.; Storer, R. I.; Taylor, S. *J. Chem. Soc., Perkin Trans.* **2000**, *1*, 3815−4195.

(3) *Polymer Supported Reagents Handbook*, Novabiochem Catalogue, 2001.

(4) Bayer, E. *Angew. Chem., Int. Ed. Engl.* **1991**, *30*, 113−129.

(5) Basso, A.; Evans, B.; Pegg, N.; Bradley, M. *Tetrahedron Lett.* **2000**, *41*, 3763−3767.

(6) Kato, M.; Kamigaito, M.; Sawamoto, M.; Higashimura, T. *Macromolecules* **1995**, *28*, 1721−1723. Wang, J. S.; Matyjaszewski, K. *J. Am. Chem. Soc.* **1995**, *117*, 5614−5615. Percec, V.; Barboiu, B. *Macromolecules* **1995**, *28*, 7970−7972.

(7) Miller, P. J.; Matyjaszewski, K. *Macromolecules* **1999**, *32*, 8760−8767.

(8) Tong, J. D.; Moineau, G.; Leclère, Ph.; Brédas, J. L.; Lazzaroni, R.; Jérôme, R. *Macromolecules* **2000**, *33*, 470−479.

(9) Huang, X.; Wirth, M. J. *Macromolecules* **1999**, *32*, 1694−1696.

(10) von Werne, T.; Patten, T. E. *J. Am. Chem. Soc.* **1999**, *121*, 7409−7410.

(11) Zheng, G.; Stöver, H. D. H. *Macromolecules* **2002**, *35*, 6828−6834.

(12) Wang, X.-S.; Armes, S. P. *Macromolecules* **2000**, *33*, 6640−6647. Zhang, X.; Matyjaszewski, K. *Macromolecules* **1999**, *32*, 7349−7353. Matyjaszewski, K.; Beers, K.; Kern, A.; Gaynor, G. *J. Polym. Sci., Part A: Polym. Chem.* **1998**, *36*, 823−830. Mecerrecyes, D.; Atthoff, B.; Boduch, K. A.; Trollsås, M.; Hedrick, J. L. *Macromolecules* **1999**, *32*, 5175−5175. Hawker, C. J.; Hedrick, J. L.; Malmström, E. E.; Trollsås, M.; Mecerrecyes, D.; Moineau, G.; Dubois, P.; Jérôme, R. *Macromolecules* **1998**, *31*, 213−219.

(13) *Polymer Handbook*, 4th ed.; Brandrup, J., Immergut, E. H., Grulke, E. A., Eds.; John Wiley & Sons: New York, 1999; p II-290.
(14) Teodorescu, M.; Matyjaszewski, K. *Macromolecules* **1999**, *32*, 4826−4831.
(15) Hu, J.; Pompe, G.; Schulze, U.; Pionteck, J. *Polym. Adv. Technol.* **1998**, *9* (10−11), 746−751.
(16) Cook, R. E.; Dainton, F. S.; Ivin, K. J. *J. Polym. Sci.* **1958**, *29*, 549−556.
(17) *The Aldrich Library of Infrared Spectra*, 3rd ed.; Pouchert, C. J., Ed.; Aldrich Chemical Co.: Milwaukee, WI, 1981; p 386F.
(18) Rademacher, J. T.; Baum, M.; Pallack, M. E.; Brittain, W. J.; Simonsick, Jr., W. J. M*acromolecules* **2000**, *33*, 284−288.

MA020421W